

Impacts of reprocessed altimetry on the surface circulation and variability of the Western Alboran Gyre

Mélanie Juza^{a,*}, Romain Escudier^a, Ananda Pascual^b, Marie-Isabelle Pujol^c,
Guillaume Taburet^c, Charles Troupin^a, Baptiste Mourre^a, Joaquín Tintoré^{a,b}

^a SOCIB, Parc Bit, Naorte, Bloc A 2° 3p, 07121 Palma de Mallorca, Spain

^b IMEDEA (UIB-CSIC), calle Miquel Marqués 21, 07190 Esporles, Spain

^c CLS, Parc Technologique du Canal, 11 rue Hermès, 31520 Ramonville-Saint-Agne, France

Received 29 January 2016; received in revised form 9 May 2016; accepted 13 May 2016

Available online 20 May 2016

Abstract

New altimetry products in semi-enclosed seas are of major interest given the importance of the coastal-open ocean interactions. This study shows how reprocessed altimetry products in the Mediterranean Sea from Archiving, Validation and Interpolation of Satellite Oceanographic data (AVISO) have improved the representation of the surface circulation over the 1993–2012 period. We focus on the Alboran Sea, which is the highest mesoscale activity area of the western Mediterranean. The respective impacts of the new mean dynamic topography (MDT) and mapped sea level anomaly (MSLA) on the description of the Western Alboran Gyre (WAG) are quantitatively evaluated. The temporal mean and variability of the total kinetic energy have been significantly increased in the WAG considering both the new MDT and MSLA (by more than 50%). The new MDT has added 39% to the mean kinetic energy, while the new MSLA has increased the eddy kinetic energy mean (standard deviation) by 53% (30%). The new MSLA has yielded higher variability of total (eddy) kinetic energy, especially in the annual frequency band by a factor of 2 (3). The MDT reprocessing has particularly increased the low-frequency variability of the total kinetic energy by a factor of 2. Geostrophic velocities derived from the altimetry products have also been compared with drifter data. Both reprocessed MDT and MSLA products intensify the velocities of the WAG making them closer to the *in situ* estimations, reducing the root mean square differences and increasing the correlation for the zonal and meridional components. The results obtained using refined coastal processing of altimetry products and new observational data are very encouraging to better understand the ocean circulation variability and coastal-open ocean interactions, and for potential improvements in other sub-basins, marginal seas and coastal global ocean.

© 2016 COSPAR. Published by Elsevier Ltd. This is an open access article under the CC BY-NC-ND license (<http://creativecommons.org/licenses/by-nc-nd/4.0/>).

Keywords: Satellite altimetry; Sea level anomaly; Mean dynamic topography; Kinetic energy; Mediterranean Sea; Western Alboran Gyre

1. Introduction

Satellite altimetry has revolutionized our vision and knowledge of ocean dynamics, providing continuous

monitoring of the sea level variability and the associated changes of the large scale surface circulation in the global ocean since the early 90s (Le Traon, 2013). Mesoscale structures are highly energetic features of the ocean circulation that interact and modify the large scale circulation at regional and local scales. The description of mesoscale variability has been enhanced with the merging of multi-mission satellites (Pascual et al., 2007). The important role of oceanic eddy dynamics in the ocean circulation, heat and salt transports, and their interactions with atmosphere and

* Corresponding author.

E-mail addresses: mjuza@socib.es (M. Juza), rescudier@socib.es (R. Escudier), ananda.pascual@imedea.uib-csic.es (A. Pascual), mpujol@cls.fr (M.-I. Pujol), gtaburet@cls.fr (G. Taburet), ctroupin@socib.es (C. Troupin), bmourre@socib.es (B. Mourre), jtintore@socib.es (J. Tintoré).

biology is now established and better understood (Morrow and Le Traon, 2012; McGillicuddy, 2016). Altimetry is also an extremely valuable tool to assess the realism of eddy permitting or resolving ocean model circulation and variability from mesoscale to interannual scale (Penduff et al., 2010; Juza et al., 2015) and to constrain ocean models through data assimilation (Mourre et al., 2006; Oke and Schiller, 2007; Bell et al., 2015). Altimetry products strongly support the operational oceanography by improving the performance of ocean modeling and forecasting systems (Le Traon et al., 2003; Haines et al., 2011; Le Traon, 2013). Better estimations and forecasts of ocean surface currents have direct applications for the pollution monitoring, marine safety, national security, marine transport, as well as coastal area and fishery managements (Tintoré et al., 2013). Additionally, altimetry has a significant impact on climate applications providing long-term series of data for the monitoring of climate signals and addressing climate variability, and also providing initial fields for coupled ocean–atmosphere models.

As a consequence of these societal and scientific applications, maximum accuracy and confidence are required in these products in both the open and coastal oceans. The continuous improvement of altimetry data corrections and processing is crucial to provide a better representation of the mesoscale variability in the global and regional oceans (Pascual et al., 2009). In recent years, the altimetry community has continued its efforts to improve the products for the global ocean and the marginal seas, both the sea level anomaly (SLA) and the mean dynamic topography (MDT), upgrading instrumental and geophysical corrections, improving interpolation methods (in particular in coastal areas; Dussurget et al., 2011; Escudier et al., 2013), calibration, satellite constellation, and geoid (e.g. exploiting data from GRACE and GOCE space gravity missions). Recent improvements in coastal altimetry have also been made (Cipollini et al., 2010; Vignudelli et al., 2011; Birol and Niño, 2015; Troupin et al., 2015). The mapped SLA (MSLA) product for the global ocean, produced and delivered by Archiving, Validation and Interpretation of Satellite Oceanographic data (AVISO, <http://www.aviso.altimetry.fr>), has been updated in 2014 (Pujol et al., 2016). Capet et al. (2014) have shown that this product improves the description of mesoscale activity in Eastern Boundary Upwelling Systems, returns higher eddy kinetic energy levels within a 300 km coastal band than the previous version (Dibarboue et al., 2011), and shows improved geostrophic velocities in coastal regions through statistical comparisons with drifter observations. Dedicated regional products have also been built and improved, such as for the Mediterranean Sea, which is a challenging area for both science and society. In this oceanic basin, the first Rossby deformation radius characterizing the minimum length of mesoscale features is around 10–15 km, four times smaller than typical values found in the world ocean (Robinson et al., 2001). The Mediterranean Sea is also a place of socio-economic and environmental concerns

related to the considerable human pressures in coastal areas and the impacts of climate change (e.g. sea level rise, marine ecosystem variations). The AVISO MSLA products for the Mediterranean Sea have also been reprocessed in 2014. Marcos et al. (2015) have evaluated the updated and previous products locally in regions close to coastal area, considering the MSLA grid points which are the closest and most correlated with the coastal tide gauge records. The comparisons with monthly values from tide gauge time series have shown that the new MSLA captures more variability, has a higher correlation in most of the selected sites, and improves the linear trends over 1993–2012.

In the western Mediterranean Sea, the Alboran Sea is particularly challenging and of great interest for the altimetry at both global and regional scales. Indeed, this region exhibits the highest energy and mesoscale activity in the basin (Pascual et al., 2014). The Atlantic Jet (AJ) enters the Alboran Sea through the Strait of Gibraltar bringing Atlantic Water into the Mediterranean Sea (Viúdez et al., 1998). The AJ modulates the main hydrographic and circulation features in this sub-basin (Baldacci et al., 2001), forming the quasi-permanent Western Alboran Gyre (WAG), the intermittent Eastern Alboran Gyre (EAG), and the strong Almeria-Oran density front, between Spain and Africa (Tintoré et al., 1988; Renault et al., 2012). The Alboran Sea is also characterized by an upwelling of nutrient rich waters along the Spanish coast north to the WAG. The fluctuations of the AJ intensity, driven by meteorological conditions, induce strong variability in these circulation features (Tintoré et al., 1991; Viúdez et al., 1998; Flexas et al., 2006). Mesoscale structures strongly affect biological processes in this sub-basin (Baldacci et al., 2001). The northern shelf region has also been shown to be a suitable area for the spawning of small pelagic fish (e.g. European anchovy or sardine; Macías et al., 2011; Ruiz et al., 2013). The high biological productivity along the Spanish coast has been found to be related to the WAG position and strength, and to enhanced lateral and vertical nutrient fluxes, declining towards the interior of the WAG (Macías et al., 2008; Oguz et al., 2014).

In this study, the new satellite absolute dynamic topography products released by AVISO are evaluated in the Alboran Sea. More precisely, we quantify the impact of both the reprocessed MDT and MSLA on the representation and variability (from weekly to interannual scales) of the WAG, which constitutes the strongest dynamical feature of the western Mediterranean mean circulation and whose position and variations directly impact the biological activity in the north-western Alboran Sea. Note that this study evaluates and quantifies the contributions of both MDT and MSLA while the previous studies assessed one of the two products. The previous and updated satellite altimetry products are compared between themselves through kinetic energy approach to evaluate the respective impacts of the MDT and MSLA updates on the mean flow and eddy variability. Additionally, the realism of the associated geostrophic velocities from altimetry is assessed

through quantitative comparisons with drifter data in the WAG area. We also propose basic diagnostics, based on medians and percentiles, to quantify the altimetry products; they complete the metrics commonly used in the altimetry community (e.g. root mean square difference and correlation).

The paper is organized as follows. Altimetry datasets and data processing are described in Section 2. The respective impact of the new MDT and MSLA products is then evaluated in terms of mean and variability in the WAG area in Section 3. Section 4 is dedicated to the assessment of the altimetry products and the quantification of their improvement using drifter data. Finally, conclusions and perspectives are given in Sections 5 and 6.

2. Absolute dynamic topography in the Mediterranean Sea

2.1. Altimetry products

The altimetry absolute dynamic topography (ADT) is computed as the sum of the sea level anomaly (SLA) and the mean dynamic topography (MDT). The surface geostrophic velocities are estimated from the satellite-derived ADT and thus their accuracy depends on the accuracy of both the SLA and MDT estimates.

New MSLA products have been released by AVISO in April 2014 for the Mediterranean Sea (Pujol et al., 2016; hereafter MSLAn for “new product”), substituting the previous products (Pujol and Larnicol, 2005; Dibarboure et al., 2011; hereafter MSLAo for “old product”). In this study, both MSLAo and MSLAn correspond to multi-mission and delayed-time (quality controlled) data which are interpolated on a regular grid of $1/8^\circ \times 1/8^\circ$ over the 1993–2012 period. A large part of the changes implemented between MSLAo and MSLAn is not specific to the Mediterranean Sea but also concerns the global ocean altimeter data processing. They are fully described in Pujol et al. (2016). We summarize here the changes, including specificities for the Mediterranean Sea processing. While the MSLAo products are weekly fields and referenced to the mean sea surface (measured by the altimeter) which is representative of the 7-year period (1993–1999), MSLAn are provided with a daily sampling and referenced to a 20 years mean sea surface (1993–2012). The time scales of variability that are resolved in MSLAn are not substantially different from MSLAo. Indeed, they are imposed by the temporal correlation function used in the optimal interpolation mapping procedure. These temporal scales used in the Mediterranean Sea are set to 10 days (Pujol and Larnicol, 2005) both for MSLAn and MSLAo. Additionally, new corrections have been applied to MSLAn. They mainly consist of new standards of instrumental and atmospheric corrections. Although many corrections were changed, the main improvements come from to the use of a new wet troposphere correction, based on ERA-interim reanalysis field, and new orbit standards (REAPER and CNES GDR-D). The details of these changes are given in

Pujol et al. (2016) and Ssalto/Duacs User Handbook (2014). The coastal data processing has also been improved in MSLAn with the use of a refined mean sea surface estimated along repetitive track, allowing the definition of SLA points closer to the coast, combined with a more restrictive selection of geodetic measurements impacted by a reduced quality of the mean sea surface near the coast (see Pujol et al., 2016). Furthermore, very short tracks previously rejected in MSLAo, have been kept in MSLAn. This last processing change has a significant impact in the Alboran Sea where only short track sections are present. The spatial extension of the MSLAn product from 4.875°W until 6°W has also significantly improved the description of the Alboran Sea. Fig. 1 illustrates the larger number of along-track data considered in MSLAn estimation due to the refined coastal data processing, the added short tracks and the spatial extension. On average 26% of MSLAn along-track data were not taken into account in MSLAo within a 40 km coastal band of the whole Mediterranean, and 28% in the Alboran Sea. Locally, the gain can reach 100%. Some tracks have been lost in the new product due to a change of orbit standard in Envisat and more stringent coastal editing on Topex-Poseidon new orbit. Locally this loss reaches 15%. Additional measurements have also been taken into account in MSLAn. Indeed, the year 2011 for the Cryosat-2 mission and the first cycles of the Jason-1 geodetic orbit have been introduced in the new product. Finally, MSLAn processing over the Mediterranean Sea also includes changes in the mapping parameters, more specifically an improved estimation of the measurement errors along the tracks of the different altimeters.

The MDT is the difference between the mean sea surface, which is measured by the altimeter, and a model geoid (where the errors are large at small scales). It represents the mean circulation over the period of reference. The MDT is estimated by combining the outputs of the Mediterranean Forecasting System model (Tonani et al., 2008, 2014) over 7 years with oceanic observations (drifting buoys and altimeter measurements). The Mediterranean MDT has also been upgraded in 2014 (Rio et al., 2014; hereafter MDTn for “new MDT”), based on the improvement of the former version (Rio et al., 2007; hereafter MDTo for “old MDT”). More precisely, extended and updated data sets spanning the 1993–2012 period (e.g. addition of hydrographic profiles from Argo floats and CTDs, extension to recent years and update of drifter data time series, update of numerical simulations) and refined procedures (e.g. data processing, new methodology) have improved the MDT product in the Mediterranean Sea, including a better description of the Alboran gyres (Rio et al., 2014).

2.2. Data processing

In this study, three datasets of mapped ADT (MADT) have been built over the 1993–2012 period in the Mediterranean Sea and compared to evaluate and quantify the

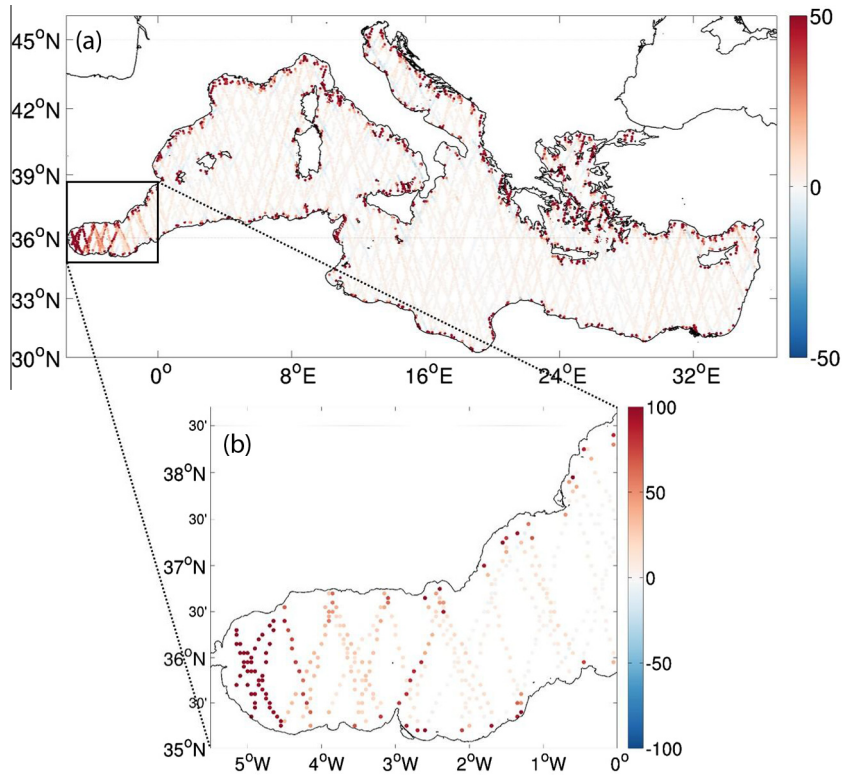


Fig. 1. Percentage of along-track SLA data in the new product which were not taken into account in the old version in the whole Mediterranean Sea (a) and in the Alboran Sea (b). Note the change of scales in color bar. Statistics are computed over 1993–2012 in $1/20^\circ \times 1/20^\circ$ boxes. The considered missions are: Topex-Poseidon (TP) and TP on its new orbit, Jason-1 (J1) and J1 on its new orbit, OSTM/Jason-2, Envisat, ERS-1, ERS-2, and Geosat Follow On. (For interpretation of the references to color in this figure legend, the reader is referred to the web version of this article.)

impact of both the new MDT and MSLA products on the representation of the WAG and its variability. The same procedures have been applied to the three MADT products for their intercomparison. The MSLAo and MSLAn products are those derived combining all available satellites (i.e. from two to four satellites at a given time). The MSLAn products, which are provided daily, have been subsampled at the dates of the MSLAo maps to match the weekly fields for their intercomparison. The three MADT datasets have been computed on the same $1/8^\circ \times 1/8^\circ$ grid as follows:

- MADToo (old MSLA + old MDT) = weekly MSLAo + MDTo (1993–1999).
- MADTon (old MSLA + new MDT) = weekly MSLAo + MDTn (1993–1999).
- MADTnn (new MSLA + new MDT) = weekly MSLAn + MDTn (1993–2012).

The MDTn has been computed over a 7-year period (1993–1999), while the MSLAn is based on a 20-year period (1993–2012). Consequently, a correction has been applied for homogeneous reference and consistency with MDTn (refer to [Ssalto/Duacs User Handbook, 2014](#)) before computing MADTnn. It consists in a temporal mean over the 7-year reference period of the MSLAn. The methodology for changing the reference period is given in [Pujol et al. \(2016\)](#) in Appendix A. Note that MADToo

(MADTnn) corresponds to the “old” (“new”) MADT product, which was (is) also provided by AVISO. The intermediate MADTon enables the MADToo-MADTon and MADTon-MADTnn comparisons to quantify the respective contributions of the MDT and MSLA product upgrades. The geostrophic velocity and associated kinetic energies will be derived from these MADT fields over the 1993–2012 period.

2.3. Total, mean and eddy kinetic energies

The MADT products are analyzed and compared between themselves through the kinetic energy in order to quantify the impact of the MDT and MSLA product updates on the mean flow and eddy variability. The geostrophic currents are estimated from the MADT products. The total kinetic energy (TKE), mean kinetic energy (MKE) and eddy kinetic energy (EKE) are computed as:

$$\text{TKE} = \frac{1}{2}(U_g^2 + V_g^2); \quad \text{MKE} = \frac{1}{2}(\overline{U_g^2} + \overline{V_g^2});$$

$$\text{EKE} = \frac{1}{2}(U_g'^2 + V_g'^2)$$

where U_g and V_g are the zonal and meridional geostrophic currents, $\overline{U_g}$ and $\overline{V_g}$ the temporal means over 1993–2012, U_g' and V_g' the anomalies with respect to $\overline{U_g}$ and $\overline{V_g}$. The

TKE represents the energy of the total surface geostrophic flow (mean and fluctuations), the MKE is the energy induced by the mean current over 1993–2012, and the EKE is representative of the mesoscale variability and allows identifying regions with high variability such as current meanders, eddies, or fronts.

The temporal mean of TKE from MADTnn over 1993–2012 highlights strong energetic ocean features in the whole Mediterranean Sea (Fig. 2a). In the western basin, the principal circulation paths are the Alboran Gyres (WAG and EAG), the Algerian Current (from 0° along the African coast), the Southerly Sardinia Current (at 8°E which then splits into three branches, one entering the Tyrrhenian Sea, and two through the Sicily Strait, the Sicily Strait Tunisian Current and the Atlantic Ionian Stream), and in the northern part, the western Corsica Current and the Northern Current. The western Mediterranean is also a place of strong mesoscale activity (e.g. large anticyclonic eddies in the southern part, the Northern Tyrrhenian Gyre). In the eastern Mediterranean, the main energetic features are the Cretan Passage Southern Current (along the African coast from 21° to 26°E) which then branches into the Mid-Mediterranean Jet and the Southern Levantine Current, the Cilician Current and the Asian Minor Current in the northern Levantine sub-basin, the recurrent

Ierapetra Gyre, and finally, the Eastern Adriatic Current and the Western Adriatic Coastal Current in the marginal Adriatic sub-basin.

Fig. 2b and c shows the ratios $TKE_{\text{Enn}}/TKE_{\text{Eoo}}$ and $TKE_{\text{Enn}}/TKE_{\text{En}}$ in the Mediterranean to identify and quantify the changes in the mean flow and eddy variabilities with the new MDT and MSLA products, respectively. The new MDT release intensifies the TKE especially in the western Ligurian Sea (the western Corsica Current and the Northern Current) where the increase factor is higher than 3. TKE increases are also induced in the WAG, the western Algerian Current, the Northern Tyrrhenian Gyre, the western Middle Adriatic Coastal Current, the Cilician Current and the Asian Minor Current. The new MSLA product has slightly decreased the TKE over the basin except in some areas such as the WAG, the Northern Current, the Northern and Southern Adriatic Gyres, and the Asian Minor Current, where the TKE has been increased by a factor of around 1.3–1.5. The general decrease of TKE in the rest of the Mediterranean Sea is mainly induced by the changes in mapping parameters (Section 2.1), which led to SLA gradients slightly smoother in MSLAn.

3. Ocean surface circulation and variability in the Alboran Sea

3.1. Mean circulation in the Alboran Sea

Fig. 3a shows the mean surface circulation, derived from the MADTnn, over 1993–2012 in the Alboran Sea. At the entrance to the Mediterranean Sea, the mean geostrophic velocity is around 0.4 m/s in a north-eastward direction, corresponding to the Atlantic inflow. Fed by the AJ, the quasi-permanent WAG, centered at 4.4°W with a diameter of 100 km, is distinctly captured with strong mean geostrophic velocities reaching 0.64 m/s. Farther east, the signature of the intermittent EAG appears, especially in its western part with mean geostrophic velocity of 0.45 m/s at 2.8°W. In its eastern part, the Almeria-Oran front is also highlighted with south-eastward mean velocity of 0.35 m/s, and which then joins and forms the eastward and coastal Algerian Current.

The mean surface circulation in the Alboran Sea differs in the different products (Fig. 3a–c), especially in the representation and intensity of the WAG and the Almeria-Oran front. The differences between the MADT products are now investigated and quantified through a kinetic energy viewpoint separating each component (MDT and MSLA). The study focuses on the WAG, which is the strongest mesoscale feature of the Alboran Sea and of special interest for biological processes.

3.2. Kinetic energy in the Western Alboran Gyre

The temporal mean of kinetic energies over 1993–2012 is first analyzed in Fig. 4. Associated WAG-box-averaged

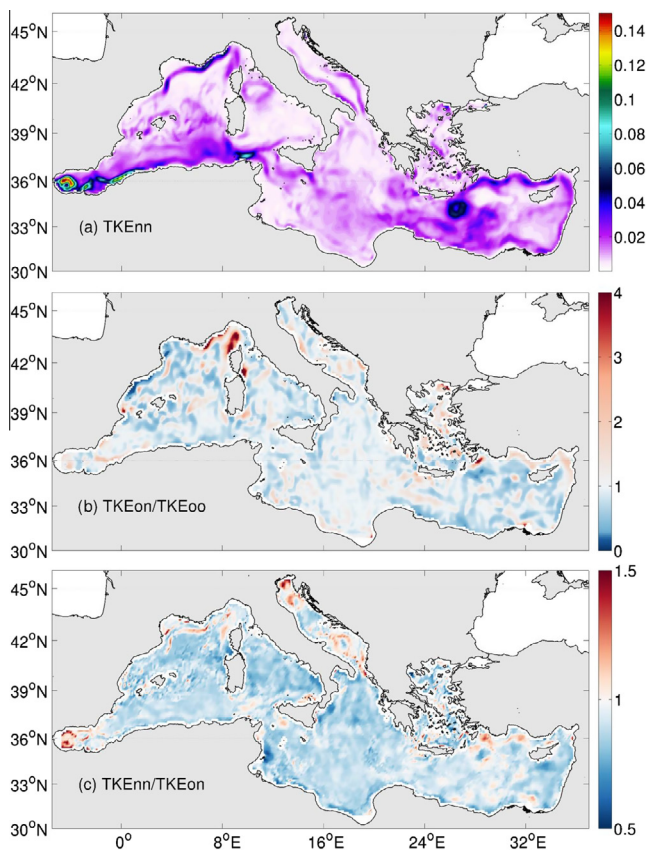


Fig. 2. Mean TKE (in m^2/s^2) derived from MADTnn over 1993–2012 in the Mediterranean Sea (a). Ratio of the mean TKE between the products over 1993–2012: $TKE_{\text{Enn}}/TKE_{\text{Eoo}}$ (b) and $TKE_{\text{Enn}}/TKE_{\text{En}}$ (c).

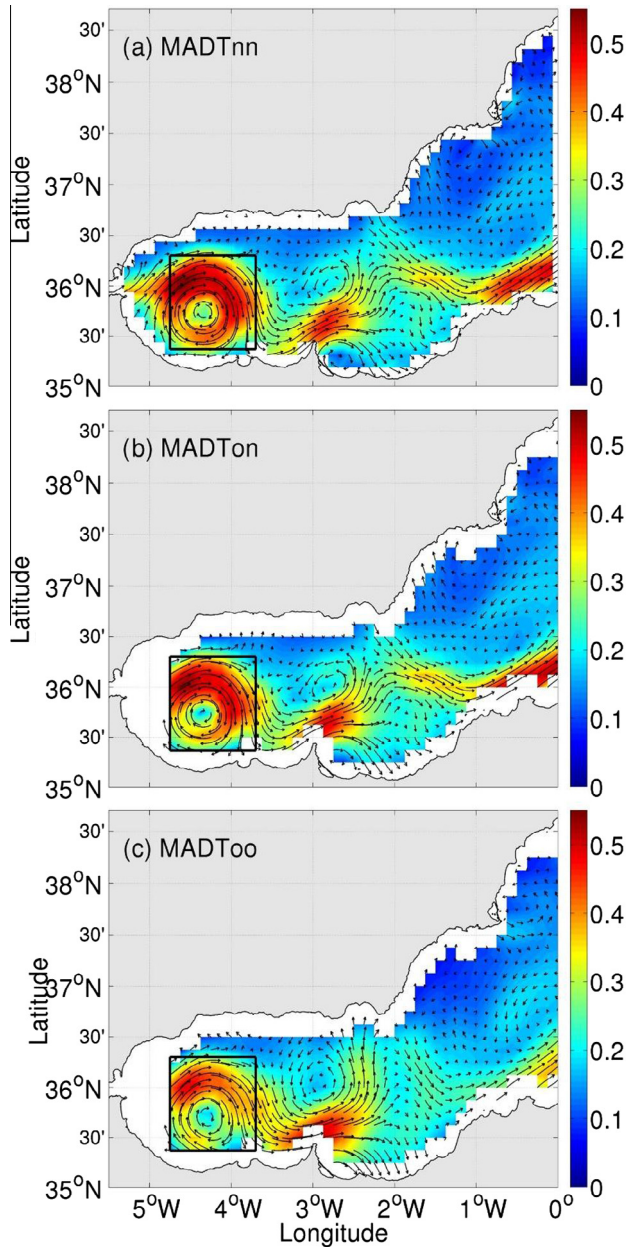


Fig. 3. Mean geostrophic velocity from MADTnn, MADTon, and MADToo over 1993–2012 in the Alboran Sea (in m/s). The black box indicates the WAG area used in Section 3.2.

values are given in Table 1. The mean TKE in the WAG area is higher in MADTnn than in MADToo and MADTon (Fig. 4a–c), reaching its maximum of $0.17 \text{ m}^2/\text{s}^2$ in the north-western part of the gyre and with a WAG-box-averaged value of $0.1 \text{ m}^2/\text{s}^2$. Both the new MDT and MSLA products increase the TKE, especially in the WAG. The TKE added value, averaged in the WAG-box, is 30% and 16% with the new MDT and MSLA, respectively. The MKE is stronger in MADTon than in MADToo (Fig. 4d and e), with an increase of 39% in the WAG-box with the new MDT. Decreased MKE values with the new MDT are also highlighted in the central area of the Alboran Sea, east of the WAG (at $3.5\text{--}3^\circ\text{W}$), and

near the southern and northern shelves (at $2.5\text{--}3^\circ\text{W}$ and 2.5°W , respectively) due to a repositioning of the WAG and EAG mean locations in the new product. Note that the MKE from MADTon and MADTnn are slightly different (Fig. 4f) because the MDT is not computed over the same period (Section 2). Concerning the EKE, the mean value is significantly increased in the new MSLA product comparing to the old one (Fig. 4g and i). The mean WAG-box-averaged EKE is higher in MADTnn ($0.023 \text{ m}^2/\text{s}^2$) than in MADToo and MADTon ($0.015 \text{ m}^2/\text{s}^2$), with an added value of 53%.

The temporal variability of kinetic energies within the WAG is also examined. The WAG box-averaged standard deviations of TKE over the period of study (Table 1) indicate increases from 0.031 to $0.036 \text{ m}^2/\text{s}^2$ (16% added) with the new MDT and from 0.036 to $0.048 \text{ m}^2/\text{s}^2$ (33% added) with the new MSLA product, considering the new MDT. This increase of variability corresponds to a more marked and higher seasonal variability in the new MSLA product. Indeed, the time series of WAG-box-averaged TKE (zoom over 2009–2012 for clarity, Fig. 5a) displays an annual cycle in the three products, with highest values in MADTnn, especially during the strongest phase of high TKE, in summer. Additionally, the spectrum of TKE (Fig. 5c) shows that the highest frequency band of variability over 1993–2012 corresponds to the annual peak, which is stronger in MADTnn than in MADTon and MADToo by a factor of 2. A peak is also revealed at the frequency of 100 weeks associated with a biannual variability: the new MDT and MSLA products increase the TKE by a factor of 2 and 1.5, respectively, at this frequency. At low-frequency variability from 4 to 20 years, the new MDT is more energetic and increases significantly the TKE by a factor of 2. Concerning the EKE, only the MSLA update impacts on the variability (same results from MADToo and MADTon, Fig. 5b and d). The new MSLA product leads to a significant increase of the WAG-box EKE standard deviation of more than 30% (from 0.013 to $0.017 \text{ m}^2/\text{s}^2$). The time series of WAG-box-averaged EKE over 2009–2012 (Fig. 5b) show stronger peaks (events) in MADTnn. This can be explained by the short tracks included in MSLA and the geographical extension of the spatial coverage until 6°W in the new product. The spectrum of EKE (Fig. 5d) also displays an annual signal and higher energy in the new MSLA product than in the previous version with a factor of 3. The low-frequency variability (with period longer than 4 years) of the EKE is also increased by a factor of 2 with the new MSLA product.

4. Comparison with drifters

Both the new MDT and MSLA products from AVISO increase the kinetic energy components in the WAG, in terms of mean and variability. In order to assess the improvement of the accuracy of reprocessed products, the three MADT datasets are compared to drifter data. In the Mediterranean Sea, the drifter data are collected,

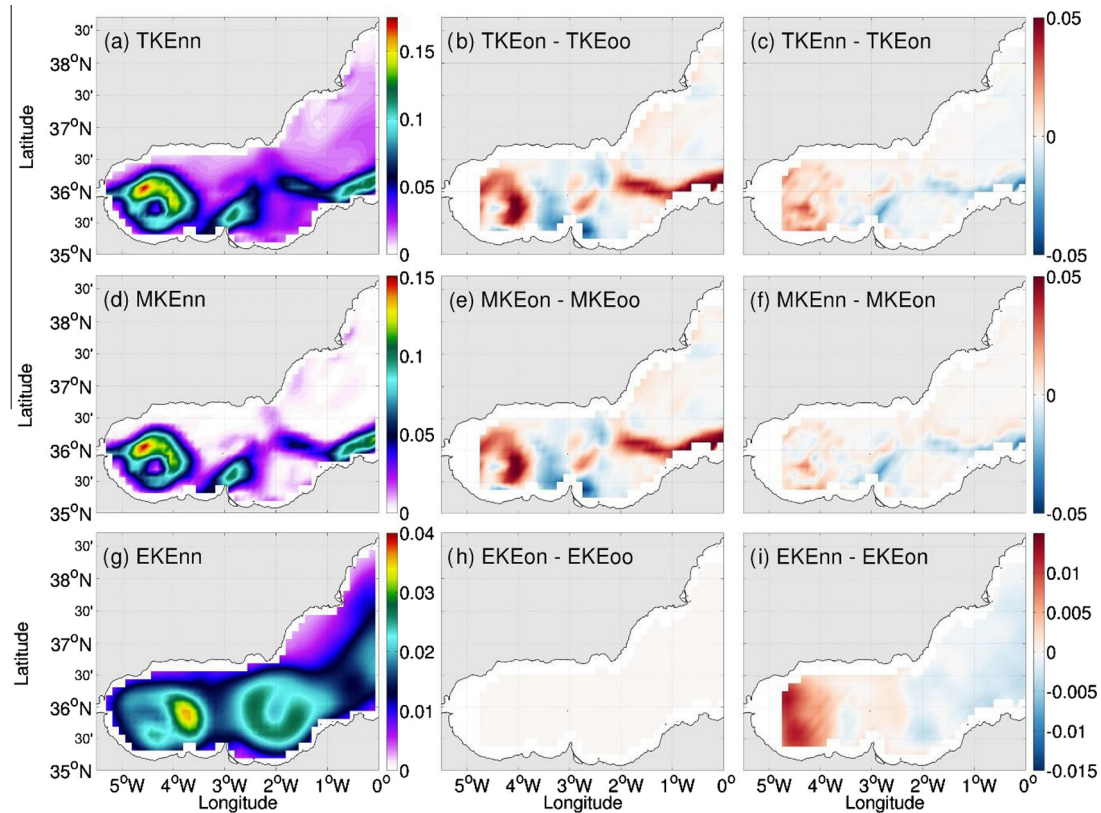


Fig. 4. Temporal means of TKE, MKE and EKE (in m^2/s^2) derived from MADTnn over 1993–2012 (a, d, g). Associated differences between MADTnn and MADTnnn (b, e, h) and between MADTnn and MADTnnn (c, f, i). Note the change of scales in TKE, MKE and EKE diagnostics for clarity.

Table 1

Temporal means of TKE, MKE, EKE, and standard deviations of TKE and EKE averaged in the WAG-box (from 4.75° to 3.7°W and from 35.4° to 36.3°N) over 1993–2012 (in m^2/s^2).

AVISO products	TKE mean	MKE	EKE mean	TKE std	EKE std
MADTnn	0.0659	0.0511	0.0148	0.0309	0.0129
MADTnnn	0.0860	0.0712	0.0148	0.0358	0.0129
MADTnnnn	0.1010	0.0785	0.0225	0.0476	0.0165

processed, quality controlled, validated and distributed by the Mediterranean Surface Velocity Program (<http://nettuno.ogs.trieste.it/sire/medsvp/>). The positions and velocities of the drifters were interpolated at regular time intervals, low-pass filtered at 36 h to remove high-frequency motions and subsampled every 6 h. We also estimated and removed the Ekman component from the drifter velocities using linear regressions with local wind data (Poulain et al., 2012). Cross-calibrated, multi-platform ocean surface wind velocity products were downloaded from the NASA Physical Oceanography Distributed Active Archive Center (PO.DAAC) during the drifter periods. The 6-hourly and $\frac{1}{4}^\circ$ gridded analyses were used (Atlas et al., 2011). Only the drifters going around the WAG during the period of study have been selected. They were deployed at different months and years (April and August 1993, April and July 1996, and November 1998), monitoring multiple events. Additionally, the drifter positions out of the WAG have been removed from the analysis to focus

on the evaluation of the WAG. The five selected drifters have a duration varying from 2 to 7 weeks in the WAG. Their trajectories are displayed in Fig. 6. The surface geostrophic velocities derived from the three MADT datasets have been interpolated in space and time at the drifter positions. The collocated velocities from drifter data and the MADT products (MADTnn, MADTnnn and MADTnnnn) are compared where the data are available for the 4 datasets, i.e. inside the smallest spatial coverage of the altimetry data (corresponding to the mask of MSLAo, displayed in Fig. 6).

Fig. 7 displays the associated boxplot of velocities for each dataset: on each box, the central line is the median, the edges of the box are the 25th and 75th percentiles, and the whiskers extend to the most extreme data points not considered outliers. The median drifter velocity is 0.53 m/s with 25th and 75th percentile values of 0.44 and 0.64 m/s, respectively. The three MADT datasets have weaker velocity than the drifter data. The differences can

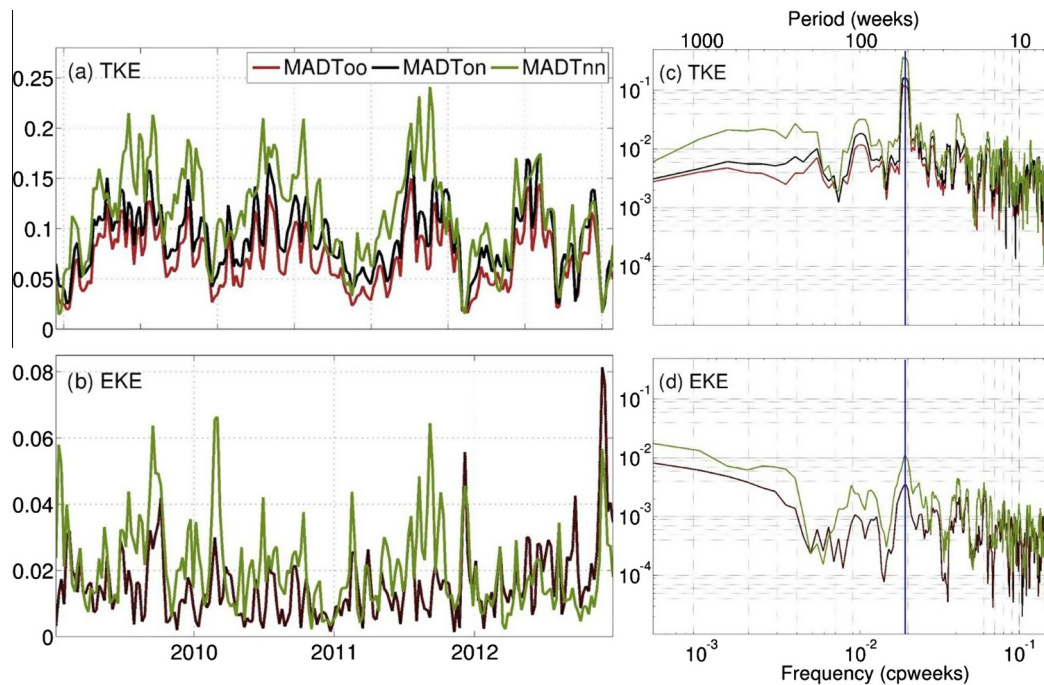


Fig. 5. Time series of TKE (a) and EKE (b) (in m^2/s^2) in the WAG-box over 2009–2012 from MADTnn, MADTon, and MADToo (green, black and red lines, respectively). Associated spectra over the whole period 1993–2012 with a zoom from 6-week period for clarity (c and d). The blue line indicates the annual peak (52 weeks). (For interpretation of the references to color in this figure legend, the reader is referred to the web version of this article.)

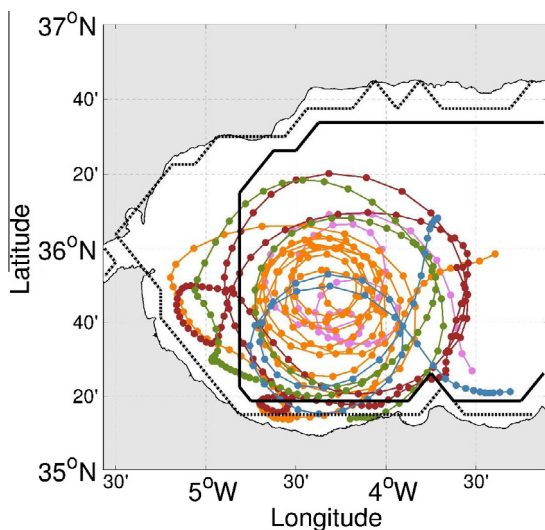


Fig. 6. Trajectory of the five selected drifters around the WAG in May 1993 (green), September 1993 (pink), April–May 1996 (orange), July–August 1996 (red) and November–December 1998 (blue). The spatial coverages of the MSLAo and MSLAn products are indicated in solid and dotted black lines, respectively. (For interpretation of the references to color in this figure legend, the reader is referred to the web version of this article.)

be partly attributed to cyclostrophic effects, corresponding to the centrifugal force on the drifter. The geostrophic velocities based on sea level slightly underestimate (overestimate) velocity in anticyclonic (cyclonic) eddies (Maximenko and Niiler, 2006). Additionally, the spatial smoothing applied to the altimetry products may explain

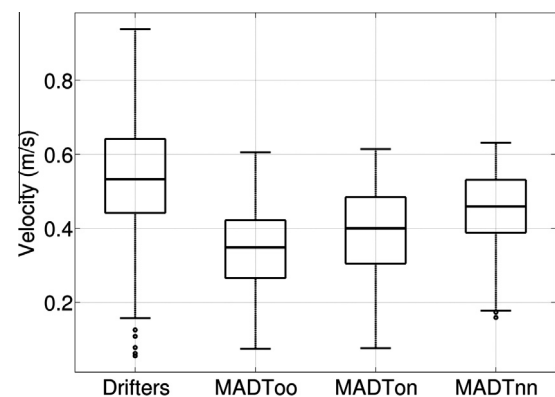


Fig. 7. Boxplot of the velocity from drifters, MADToo, MADTon and MADTnn: medians (grey line), 25th and 75th percentiles (box), 5th and 95th percentiles (black line).

their lower velocities. However, both the new MDT and MSLA products lead to an increased intensity, which is closer to the drifter estimates. The median value of the altimetry geostrophic velocity is increased from 0.35 to 0.4 m/s with the new MDT, and from 0.4 to 0.46 m/s with the new MSLA product. The too weak median values in the altimetry are mainly due to the high drifter velocities which are not well represented in the altimetry products rather than errors in other velocity bands or a general shift in the whole velocity range. Indeed, the 95th percentiles are largely smaller in altimetry (0.52, 0.56 and 0.59 m/s in MADToo, MADTon, MADTnn, respectively) than in drifters (0.8 m/s) while the 5th percentiles differ less (0.15,

0.19, 0.26 and 0.27 m/s values for MADToo, MADTon, MADTnn and drifters, respectively). However, the geostrophic velocities from MADToo and MADTon, i.e. including the MSLAo product, have too weak velocities, highlighted by the 5th and 25th percentiles which are smaller in MADToo and MADTon than in drifters. The new MSLA product performs better than old product with higher lowest values, and 5th and 25th percentiles. Finally, it should be noted that the periods of the selected drifters correspond to periods merging two satellite altimeter missions at a given time to produce SLA maps; as shown in Pascual et al. (2007), a better agreement between altimetry and drifter data can be expected with more missions available, combining three or four altimeters.

The velocity is then decomposed into its zonal (U) and meridional (V) components, from which the standard deviations, root mean square differences (RMSD) and correlations between altimetry and drifter data are computed. The results are represented in a Taylor diagram (Taylor, 2001), which is displayed in Fig. 8, combining the five drifter time series (for clarity since every individual drifter time series leads to the same conclusions). The standard deviation of U (V) is higher in the drifter data than in the altimetry products with values of 0.41 (0.38 m/s). Both the new MDT and MSLA products increase the variability of the two velocity components. The standard deviations of U (V) are around 0.24, 0.28 and 0.32 m/s (0.25, 0.27, and 0.31 m/s) for MADToo, MADTon, and MADTnn, respectively. The new MDT product reduces slightly the RMSD of U (V) from 0.25 to 0.22 m/s (from 0.19 to 0.18 m/s) and increases slightly the correlation with the drifter data from 0.84 to 0.86 (from 0.89 to 0.9). Larger improvements are found with the new MSLA product which decreases the RMSD for U (V) from 0.22 to 0.17 m/s (from 0.18 to

0.14 m/s) and increases the correlation with drifters for U (V) from 0.86 to 0.92 (from 0.9 to 0.93). In conclusion, the new MDT and MSLA products improve the intensity and variability of the WAG. Additionally, the new MSLA product benefits from a more spatially extended field (as displayed in Fig. 6), which has not been examined in this study since the same mask has been applied to all datasets for their intercomparison.

5. Conclusions

In this study, recently released satellite altimetry products from AVISO have been assessed in a marginal Sea (the Mediterranean Sea), especially in a region close to coastal area (the Alboran Sea) and where previous studies have shown an important contribution of mesoscale activity to the biological production. In particular, the impact of both MDT and MSLA updates on the representation of the WAG has been evaluated and quantified. The MDT, which was updated in 2014, was improved through the extension and update of the observational (drifters, hydrographic data) and numerical datasets, as well as refined data processing. The main modifications applied to the MSLA in 2014 for the Mediterranean Sea are the larger number of data taken into account in the new product (consideration of short tracks and geographical extension until 6°W), a better selection of data near the coast along the repetitive tracks, as well as a better estimation of the errors along the tracks.

This paper shows the new MDT and MSLA products yield levels of total kinetic energy 30% and 16%, respectively, higher than the old products in the WAG area. The new MDT increases the mean kinetic energy by 39% while the new MSLA product increases significantly the eddy kinetic energy in the WAG with an added value of 53%. The spectral content of the new MSLA in the area also displays higher levels of both total and eddy kinetic energies, especially in the annual frequency band. Additionally, quantitative assessment of the geostrophic velocity estimated from the altimetry products has been performed using drifter data, advected by the WAG during the period of study. The velocity fields derived from reprocessed MDT and MSLA products are in better agreement with *in situ* estimates in terms of mean and variability. The median value of the geostrophic velocities has been increased with the new products. The associated percentage errors have been reduced from 34% to 25% with the new MDT, and from 25% to 13% with the new MSLA. The whole range of velocities has been improved, although most of important errors in the reprocessed MADT remain in the high velocity band. This study also shows both the zonal and meridional components have been improved with the new MDT and MSLA, with an increased variability (reducing by half the error on the U and V standard deviations), a decreased RMSD of U (V) by 30% (26%) and a higher correlation. In conclusion, the present study demonstrates that the newly

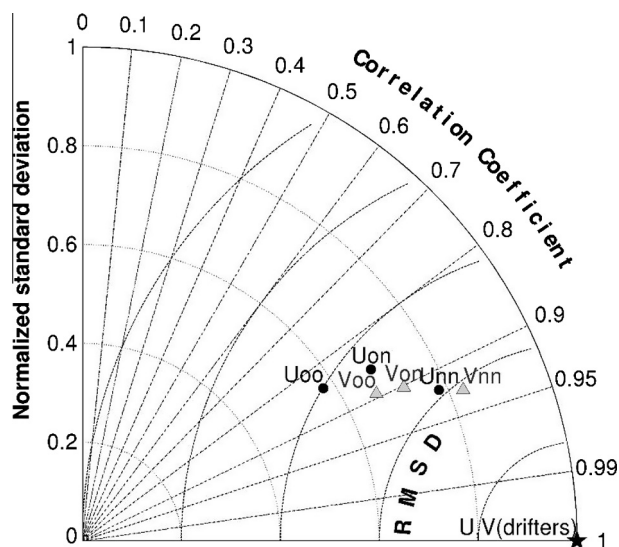


Fig. 8. Taylor diagram for the zonal (U) and meridional (V) velocities (black points and grey triangles, respectively) between drifters and altimetry products (MADToo, MADTon and MADTnn).

altimetry products, both the MDT and MSLA, enhance the description of the WAG (intensity and variability).

6. Perspectives

While this assessment focuses on the Alboran Sea, we have also evidenced (Fig. 2) that reprocessing MDT and MSLA also affects the TKE in other regions of the Mediterranean. For example, we have shown significant increases of TKE with the new MDT which improves the representation of the western Algerian Current, the Liguro-Provençal Current, the Northern Tyrrhenian Gyre, the western Adriatic Current, the Cilician Current and the Asian Minor Current. Additionally, the increased number of data near the coast and the better coastal description in the new MSLA product also contribute to a better representation of the Northern Current in the north-western Mediterranean Sea in terms of intensity, width, and variations. Through the larger number of along-track data and refined data processing, improvements are also expected in other coastal regions such as the Adriatic Sea (cyclonic gyres) and the northern Levantine basin (Asian Minor Current), where differences of TKE have been found between the MSLA products.

Therefore, the newly reprocessed altimetry products would provide a better characterization of ocean circulation and its variability in other coastal to open ocean regions worldwide, contributing as a result to a better understanding of the interactions between mesoscale and large scale variability, boundary currents and shelf areas, and physical and biological processes. In other words, this study proves that continuous improvement of data processing in altimetry and of the number of along-track data are crucial for a correct monitoring and a better description of surface circulation and mesoscale variability.

The world oceans and their marginal seas are important environmental and recreational assets. Our knowledge of the past and present as well as our capacity to predict the future could provide information to support decision making for a sustainable economic growth aligned with the environmental challenges. The progress in operational oceanography will be supported by the use of multiplatform integrated observing systems, new technologies and observations, assuring the data quality, as well as a sustained monitoring and multi-year products. The sustainability and reliability of altimetry data remain a challenge in the space and oceanography communities and efforts have to be continued. The SARAL/AltiKa satellite, launched in 2013, allows getting closer to the coast and provides a better representation of the ocean dynamics in the coastal zones. Jason-3 has been launched in January 2016 and will ensure the continuity of Topex-Poseidon and Jason-1/2 long time series. The Sentinel-3 mission, which has been launched in February 2016, will provide data continuity for the ERS, Envisat and SPOT satellite. The NASA/CNES/ESA Surface Water Ocean Topography

(SWOT) mission, which is scheduled for launch in 2020, aims to improve both spatial resolution and sea surface height precision. The data processing (e.g. calibration, editing, geophysical corrections, validation, filtering, and interpolation methods) also carries on to be challenging. It will need to be improved and adapted to higher resolution data, coastal areas, as well as new and future mission characteristics.

Acknowledgments

We gratefully acknowledge the three anonymous reviewers for their relevant remarks. The study has been conducted using altimetry data, which are produced by Ssalto/Duacs and distributed by AVISO, with support from CNES (<http://www.aviso.altimetry.fr/duacs/>). We also acknowledge the Ssalto/Duacs team for providing valued information about the along-track data considered in the MSLA products. We thank very much Pierre-Marie Poulain and the Mediterranean Surface Velocity Program for the coordination, processing and distribution of drifter data in the Mediterranean Sea. This paper is a contribution to Medclis program, a collaboration between “la Caixa” Foundation and SOCIB, and also to the Sea Level Thematic Assembly Center (SLTAC) of the Copernicus Marine Environment Monitoring Service (CMEMS).

References

- Atlas, R., Hoffman, R.N., Ardizzone, J., Leidner, S.M., Jusem, J.C., Smith, D.K., Gombos, D., 2011. A cross-calibrated, multiplatform ocean surface wind velocity product for meteorological and oceanographic applications. *Bull. Am. Meteorol. Soc.* 92 (2), 157–174. <http://dx.doi.org/10.1175/2010BAMS2946.1>.
- Baldacci, A., Corsini, G., Grasso, R., Manzella, G., Allen, J.T., Cipollini, P., et al., 2001. A study of the Alboran sea mesoscale system by means of empirical orthogonal function decomposition of satellite data. *J. Mar. Syst.* 29 (1–4), 293–311. [http://dx.doi.org/10.1016/S0924-7963\(01\)00021-5](http://dx.doi.org/10.1016/S0924-7963(01)00021-5).
- Bell, M.J., Schiller, A., Le Traon, P.-Y., Smith, N.R., Dombrowsky, E., Wilmer-Becker, K., 2015. An introduction to GODAE OceanView. *J. Oper. Oceanogr.* 8 (sup1), s2–s11. <http://dx.doi.org/10.1080/1755876X.2015.1022041>.
- Birol, F., Niño, F., 2015. Ku- and Ka-band altimeter data in the Northwestern Mediterranean Sea: impact on the observation of the coastal ocean variability. *Mar. Geod.* 38 (sup1), 313–327. <http://dx.doi.org/10.1080/01490419.2015.1034814>.
- Capet, A., Mason, E., Rossi, V., Troupin, C., Faugère, Y., Pujol, M.-I., et al., 2014. Implications of refined altimetry on estimates of mesoscale activity and eddy-driven offshore transport in the Eastern Boundary Upwelling Systems. *Geophys. Res. Lett.* 41 (21), 7602–7610. <http://dx.doi.org/10.1002/2014GL061770>.
- Cipollini, P., Beneviste, J., Bouffard, J., Emery, W., Fenoglio-Marc, L., Gommenginger, C., 2010. The role of altimetry in coastal observing systems. In: Hall, J., Harrison, J., Stammer, D. (Eds.), *Proceedings of OceanObs'09: Sustained Ocean Observations and Information for Society*, 2. European Space Agency, pp. 181–191, WPP-306.
- Dibarboure, G., Pujol, M.-I., Birol, F., Le Traon, P.-Y., Larnicol, G., Picot, N., et al., 2011. Jason-2 in DUACS: first tandem results and impact on processing and products. *Mar. Geod.* 34 (3–4), 214–241. <http://dx.doi.org/10.1080/01490419.2011.58482>.

- Dussurget, R., Birol, F., Morrow, R., De Mey, P., 2011. Fine resolution altimetry data for a regional application in the Bay of Biscay. *Mar. Geod.* 34 (3–4), 447–476. <http://dx.doi.org/10.1080/01490419.2011.584835>.
- Escudier, E., Bouffard, J., Pascual, A., Poulain, P.-M., Pujol, M.-I., 2013. Improvement of coastal and mesoscale observation from space: application to the north-western Mediterranean Sea. *Geophys. Res. Lett.* 40 (10), 2148–2153. <http://dx.doi.org/10.1002/grl.50324>.
- Flexas, M.M., Gomis, D., Ruiz, S., Pascual, A., Leon, P., 2006. In situ and satellite observations of the eastward migration of the Western Alboran Sea Gyre. *Prog. Oceanogr.* 70 (2), 486–509. <http://dx.doi.org/10.1016/j.pocean.2006.03.017>.
- Haines, K., Lea, D., Bingham, R., 2011. Using the GOCE MDT in ocean data assimilation. Proc. of 4th International GOCE User Workshop, Munich, Germany, 31 March – 1 April (ESA SP-696, July 2011).
- Juza, M., Mourre, B., Lellouche, J.-M., Tonani, M., Tintoré, J., 2015. From basin to sub-basin scale assessment and intercomparison of numerical simulations in the western Mediterranean Sea. *J. Mar. Syst.* 149, 36–49. <http://dx.doi.org/10.1016/j.jmarsys.2015.04.010>.
- Le Traon, P.Y., Hernandez, F., Rio, M.-H., Davidson, F., 2003. How operational oceanography can benefit from dynamic topography estimates as derived from altimetry and improved geoid. *Space Sci. Rev.* 108 (1–2), 239–249.
- Le Traon, P.Y., 2013. From satellite to Argo and operational oceanography: three revolutions in oceanography. *Ocean Sci.* 9 (5), 901–915. <http://dx.doi.org/10.5194/os-9-901-2013>.
- Macías, D., Bruno, M., Echevarría, F., Vázquez, A., García, C.M., 2008. Meteorologically induced mesoscale variability of the North-western Alboran Sea (southern Spain) and related biological patterns. *Estuarine Coastal Shelf Sci.* 78 (2), 250–266. <http://dx.doi.org/10.1016/j.ecss.2007.12.008>.
- Macías, D., Catalán, I.A., Solé, J., Morales-Nin, B., Ruiz, J., 2011. Atmospheric-induced variability of hydrological and biogeochemical signatures in the NW Alboran Sea. Consequences for the spawning and nursery habitats of European anchovy. *Deep Sea Res. Part I* 58 (12), 1175–1188. <http://dx.doi.org/10.1016/j.dsr.2011.08.013>.
- Marcos, M., Pascual, A., Pujol, M.-I., 2015. Improved satellite altimeter mapped sea level anomalies in the Mediterranean Sea: a comparison with tide gauges. *Adv. Space Res.* 56 (4), 596–604. <http://dx.doi.org/10.1016/j.asr.2015.04.027>.
- Maximenko, N., Niiler, P.P., 2006. Mean surface circulation of the global ocean inferred from satellite altimeter and drifter data. 15 years of Progress in Radar Altimetry. ESA Publication SP-614.
- McGillicuddy Jr., D.J., 2016. Mechanisms of physical-biological-biogeochemical interaction at the ocean mesoscale. *Mar. Sci.* 8 (1), 125–159. <http://dx.doi.org/10.1146/annurev-marine-010814-015606>.
- Morrow, R., Le Traon, P.-Y., 2012. Recent advances in observing mesoscale ocean dynamics with satellite altimetry. *Adv. Space Res.* 50 (8), 1062–1076.
- Mourre, B., De Mey, P., Ménard, Y., Lyard, F., Le Provost, C., 2006. Relative performance of future altimeter systems and tides gauges in constraining a model of North Sea high-frequency barotropic dynamics. *Ocean Dyn.* 56 (5–6), 473–486. <http://dx.doi.org/10.1007/s10236-006-0081-2>.
- Oguz, T., Macías, D., Garcia-Lafuente, J., Pascual, A., Tintoré, J., 2014. Fueling plankton production by a meandering frontal jet: A CASE STUDY for the Alboran Sea (Western Mediterranean). *PLoS One* 9 (11), e111482. <http://dx.doi.org/10.1371/journal.pone.0116653>.
- Oke, P.R., Schiller, S., 2007. Impact of Argo, SST and altimeter data on an eddy-resolving ocean reanalysis. *Geophys. Res. Lett.* 34 (19), L19601.
- Pascual, A., Pujol, M.-I., Larnicol, G., Le Traon, P.Y., Rio, M.H., 2007. Mesoscale mapping capabilities of multi-satellite altimeter mission: first results with real data in the Mediterranean Sea. *J. Mar. Syst.* 65 (1–4), 190–2011.
- Pascual, A., Boone, C., Larnicol, G., Le Traon, P.Y., 2009. On the quality of real-time altimeter gridded fields: comparison with in situ data. *J. Atmos. Oceanic Technol.* 26 (3), 556–569. [10.1175/2008JTECH0556.1](http://dx.doi.org/10.1175/2008JTECH0556.1).
- Pascual, A., Vidal-Vijande, E., Ruiz, S., Somot, S., Papadopoulos, V., 2014. Spatiotemporal Variability of the Surface Circulation in the Western Mediterranean: A Comparative Study Using Altimetry and Modeling, first ed. In: Eusebi Borzelli, Gian Luca, Gacic, Miroslav, Lionello, Piero, Malanotte-Rizzoli, Paola (Eds.), *The Mediterranean Sea: Temporal Variability and Spatial Patterns*, Geophysical Monograph 202. John Wiley and Sons, Inc.
- Penduff, T., Juza, M., Brodeau, L., Smith, G.C., Barnier, B., Molines, J.-M., et al., 2010. Impact of global ocean model resolution on sea-level variability with emphasis on interannual time scales. *Ocean Sci.* 6 (1), 269–284.
- Poulain, P., Menna, M., Mauri, E., 2012. Surface geostrophic circulation of the Mediterranean Sea derived from drifter and satellite altimeter data. *J. Phys. Oceanogr.* 42 (6), 973–990. <http://dx.doi.org/10.1175/JPO-D-11-0159.1>.
- Pujol, M.-I., Larnicol, G., 2005. Mediterranean Sea eddy kinetic energy variability from 11 years of altimetric data. *J. Mar. Syst.* 58 (3–4), 121–142.
- Pujol, M.-I., Faugère, Y., Taburet, G., Dupuy, S., Pelloquin, C., Ablain, M., et al., 2016. DUACS DT2014: the new multi-mission altimeter dataset reprocessed over 20 years. *Ocean Sci. Discuss.* <http://dx.doi.org/10.5194/os-2015-110>, under review.
- Renault, L., Oguz, T., Pascual, A., Vizoso, G., Tintoré, J., 2012. Surface circulation in the Alboran Sea (western Mediterranean) inferred from remotely sensed data. *J. Geophys. Res. Oceans* 117 (C8). <http://dx.doi.org/10.1029/2011JC007659>.
- Rio, M.-H., Poulain, P.-M., Pascual, A., Mauri, E., Larnicol, G., Santoleri, R., 2007. A mean dynamic topography of the Mediterranean Sea computed from altimetric data, in-situ measurements and a general circulation model. *J. Mar. Syst.* 65 (1–4), 484–508. <http://dx.doi.org/10.1016/j.jmarsys.2005.02.006>.
- Rio, M.-H., Pascual, A., Poulain, P.-M., Menna, M., Barceló, B., Tintoré, J., 2014. Computation of a new mean dynamic topography for the Mediterranean Sea from model outputs, altimeter measurements and oceanographic in situ data. *Ocean Sci.* 10, 731–744. <http://dx.doi.org/10.5194/os-10-731-2014>.
- Robinson, A.R., Leslie, W.G., Theocharis, A., Lascaratos, A., 2001. Mediterranean sea circulation. *Encyclopedia of Ocean Sciences*, 3. Academic, London, pp. 1689–1705. <http://dx.doi.org/10.1006/rwos.2001.0376>.
- Ruiz, J., Macías, D., Rincón, M.M., Pascual, A., Catalán, I.A., Navarro, G., 2013. Recruiting at the edge: kinetic energy inhibits anchovy populations in the Western Mediterranean. *PLoS One* 8 (2), e55523. <http://dx.doi.org/10.1371/journal.pone.0055523>.
- Ssalto/Duacs User Handbook: M(SLA) and M(ADT) Near-Real Time and Delayed-Time, 2014. SALP-MU-P-EA-21065-CLS, 4.1 edition, May 2014. Available at <http://www.aviso.altimetry.fr/fileadmin/documents/data/tools/hdbk_duacs.pdf> (last access 07.12.15).
- Taylor, K.E., 2001. Summarizing multiple aspects of model performance in a single diagram. *J. Geophys. Res. Atmos.* 106 (D7), 7183–7192.
- Tintoré, J., La Violette, P.E., Blade, I., Cruzado, A., 1988. A study of an intense density front in the Eastern Alboran Sea: the Almeria-Oran front. *J. Phys. Oceanogr.* 18, 1384–1397.
- Tintoré, J., Gomis, D., Alonso, S., 1991. Mesoscale dynamics and vertical motion in the Alboran Sea. *J. Phys. Oceanogr.* 21, 811–823.
- Tintoré, J., Vizoso, G., Casa, B., Heslop, E., Pascual, A., Orfila, A., et al., 2013. SOCIB: the Balearic Islands coastal ocean observing and forecasting system responding to science, technology and society needs. *Mar. Technol. Soc. J.* 47 (1), 101–117.
- Tonani, M., Pinardi, N., Dobricic, S., Pujol, M.-I., Fratianni, C., 2008. A high-resolution free-surface model of the Mediterranean Sea. *Ocean Sci.* 4 (1), 1–14.
- Tonani, M., Teruzzi, A., Korres, G., Pinardi, N., Crise, A., Adani, M., et al., 2014. The Mediterranean monitoring and forecasting centre, a component of the MyOcean system. In: Dahlin, H., Fleming, N.C., Petersson, S.E. (Eds.), *Proceedings of the 6th International Conference on EuroGOOS* 4–6 October 2011. Eurogoos Publication,

- Sopot, Poland, ISBN 978-91-974828-9-9 (First published 2014. No. 30).
- Troupin, C., Pascual, A., Valladeau, G., Pujol, I., Lana, A., Heslop, E., et al., 2015. Illustration of the emerging capabilities of SARAL/AltiKa in the coastal zone using a multi-platform approach. *Adv. Space Res.* 55 (1), 51–59. <http://dx.doi.org/10.1016/j.asr.2014.09.011>.
- Vignudelli, S., Kostianoy, A., Cipollini, P., Benveniste, J. (Eds.), 2011. *Coastal Altimetry*. Springer, ISBN 978-3-642-12795-3. <http://dx.doi.org/10.1007/978-3-642-12796-0>.
- Viúdez, A., Pinot, J.-M., Haney, R.L., 1998. On the upper circulation in the Alboran Sea. *J. Geophys. Res.* 103 (C10), 21653–21666.
- EAG*: Eastern Alboran Gyre
EKE: eddy kinetic energy
MADT: mapped absolute dynamic topography
MDT: mean dynamic topography
MKE: mean kinetic energy
MSLA: mapped sea level anomaly
RMSD: root mean square difference
SLA: sea level anomaly
TKE: total kinetic energy
WAG: Western Alboran Gyre

Glossary

ADT: absolute dynamic topography
AJ: Atlantic Jet
CTD: conductivity, temperature, and depth